

Luminescent Closed Shell Nickel(II) Pyridyl-azo-oximates and the Open Shell Anion Radical Congener: Molecular and Electronic Structure, Ligand Redox and Biological Activity

Shuvam Pramanik,^a Suhana Dutta,^b Sima Roy,^a Soumitra Dinda,^{a,b} Tapas Ghorui,^a Arup Kumar Mitra,^b Kausikisankar Pramanik*^a and Sanjib Ganguly*^b

^a*Department of Chemistry, Inorganic Chemistry Section, Jadavpur University, Kolkata – 700032, India.*

E-mail: kpramanik@hotmail.com, Tel: +9133 2457 2781

^b*Department of Chemistry, St. Xavier's College, Kolkata – 700016, India.*

E-mail: icsgxav@gmail.com Tel: +9133 2255 1266

Experimental details

Physical measurements

¹H NMR spectra were measured on a Bruker FT 300 MHz spectrometer. Elemental analyses (C, H, N) were performed on a PerkinElmer 2400 series II analyzer. The electro-analytical instrument, BASi Epsilon-EC for cyclic voltammetric experiments in acetonitrile solutions containing 0.2 M tetrabutylammonium hexafluorophosphate as supporting electrolyte, was used. The BASi platinum working electrode, platinum auxiliary electrode, and Ag/AgCl reference electrode were used for the measurements. The electronic spectra in dichloromethane solution were obtained using a Perkin-Elmer LAMDA 25 spectrophotometer with a solute concentration of about 10⁻⁵ M. Emission spectra were recorded on Horiba FluoroMax-4 spectrometer in deaerated dichloromethane solutions at room temperature. Emission quantum yields of the complexes were determined in deaerated solutions of the complexes by a relative method using 2-aminopyridine in 0.1 N H₂SO₄ as the standard.¹ The emission quantum yield (Φ_r) and radiative (k_r) and nonradiative (k_{nr}) decay rate constants for complexes was calculated by the equations given below:²

$$\Phi_r = \Phi_{std} \frac{A_{std} I_r \eta_r^2}{A_r I_{std} \eta_{std}^2} \quad (1)$$

$$k_r = \frac{\Phi}{\tau} \quad (2)$$

$$k_{nr} = \frac{1 - \Phi}{\tau} \quad (3)$$

where Φ_r and Φ_{std} are the quantum yields of unknown and standard samples ($\Phi_{std} = 0.60$ for 2-Aminopyridine), A_r and A_{std} are the solution absorbance at the excitation wavelength (λ_{ex}), I_r and I_{std} are the integrated emission intensities, and η_r and η_{std} are the refractive indices of the solvents. For all luminescence measurements excitation and emission slit widths of 2 nm was used. Quantum yields of complexes were determined at 25 °C in freeze–pump–thaw degassed solutions of dichloromethane. Time-correlated single-photon counting (TCSPC) measurements were carried out for the luminescence decay of complexes in dichloromethane. For TCSPC measurement, the photoexcitation was made at 300nm for ligand **1** and 330 nm for the complexes **2** and **3** using a picosecond diode laser (IBH Nanoled-07) in an

IBH Fluorocube apparatus. The fluorescence decay data were collected on a Hamamatsu MCP photomultiplier (R3809) and were analyzed by using IBH DAS6 software. Electron paramagnetic resonance (EPR) spectra were recorded in standard quartz EPR tubes using JEOL JES-FA200 X-band spectrometer.

Crystallographic Studies

X-ray intensity data for compounds **2b** was measured at 298(2) K on a Bruker AXS SMART APEX CCD diffractometer Mo K α ($\lambda = 0.71073$ Å). Metal atoms were located by direct methods, and the rest of the non-hydrogen atoms emerged from successive Fourier synthesis. The structures were refined by full-matrix least-squares procedures on F^2 . The hydrogen atoms were included in calculated positions and treated as riding atoms using SHELXL default parameters. Calculations were performed using the SHELXTL V 6.14 program package.³ Thermal ellipsoids were drawn at the 50% probability level. Molecular structure plots were drawn using the Oak Ridge thermal ellipsoid plot ORTEP.⁴ Hydrogen atoms were kept fixed using the riding model during refinement for both **2** and **3**.

Computational Study

The molecular geometry of the singlet ground state (S_0) and the first excited triplet state (T_1) of the synthesized complexes **2** and **3** have been calculated by DFT method using the (U)B3LYP⁵ hybrid functional approach incorporated in GAUSSIAN 09 program package.⁶ The geometries of the complexes were fully optimized in gas phase without imposing any symmetry constraints. The nature of all the stationary points was checked by computing vibrational frequencies, and all the species were found to be true potential energy minima, as no imaginary frequency were obtained (NImag= 0). The single crystal X-ray coordinates have been used as the initial input in all calculations for **2b**. On the basis of the optimized ground and excited state geometries, the absorption and emission spectra properties in acetonitrile (CH₂Cl₂) media were calculated by the time-dependent density functional theory (TD-DFT)⁷ approach associated with the conductor-like polarizable continuum model (CPCM).⁸ The results of the TD calculations were qualitatively similar to the observed spectra. The TD-DFT approach is now well-known as a rigorous formalism for the treatment of electronic excitation energies within the DFT framework for calculating spectral properties of many transition metal complexes.⁹ Hence TD-DFT had been shown to provide a reasonable spectral feature for the compounds under investigation. Moreover, to get an insight about the ground state geometry, electronic structure and nature of FMOs of **3**, it was optimized by assuming an $S = 3/2$ spin state.

The nickel atom was described by a double- ζ basis set with the effective core potential of Hay and Wadt (LANL2DZ)¹⁰ and the modified 6-31G basis set¹¹ was used for the other elements present in the complexes to optimize the geometries. The calculated electronic density plots for frontier molecular orbitals were prepared by using the GaussView 5.0 software. GaussSum program, version 2.2¹² was used to calculate the molecular orbital contributions from groups or atoms.

Antimicrobial activity: Determination of MIC

The pyridyl-azo-oxime ligand and its synthesized nickel chelate along as well as the starting nickel acetate were evaluated for their antibacterial activity against *Staphylococcus aureus* MTCC 3160, *Streptococcus epidermidis* MTCC 9041 (as Gram-positive bacteria) *E.coli* MTCC 443 and *Pseudomonas aeruginosa*, MTCC 741 (as Gram-negative bacteria) by using turbidimetric assay method¹³. To determine the minimum inhibitory concentration (MIC). Stock concentration of each test compound was 1mM and was further diluted within the range of 1.56-50 μ M. The lowest concentration of the compound that completely inhibits bacterial growth (no turbidity) in comparison to control was regarded as MIC.¹⁴ The result of MIC from turbidity method was further confirmed by Agar cup plate method.¹⁵

Study of antibacterial mechanism of action:

Determination of bacterial motility: Bacterial motility was observed by hanging drop method using phase contrast microscope.¹³

Preparation of bacterial lysate: The bacterial cells were incubated with IC₅₀ dose of the test compounds for overnight at 37°C. Cell lysis buffer was added to the pellet and after sonication tubes were centrifuged at 10000rpm for 10minutes at 4°C. Supernatant was collected stored at -20°C for biochemical analysis. The protein in the supernatant was estimated by the Bradford assay.

Measurement of enzymatic antioxidants: Catalase (CAT) activity was determined using a reaction mixture containing 200 μ L of 40 mM H₂O₂ in a 50mM phosphate buffer (pH 7.0) and 0.1 mL of bacterial lysate in a total volume of 3 ml. The absorbance of H₂O₂ was measured at 240 nm and the activity of enzyme was expressed in units/mL.¹⁶

Superoxide dismutase(SOD): The rate of pyrogallol auto-oxidation was measured at 470 nm every 30 seconds for 5 minutes by a spectrophotometer. The activity of SOD was expressed as unit/mg protein (1 unit was the amount of enzyme that was utilized to inhibit 50% of auto-oxidation of pyrogallol/min).¹⁷

Peroxidase (Perx) activity: was determined according to Mohammadi *et al.*, 2015.¹⁸

Measurement of non-enzymatic antioxidant: Glutathione (GSH): was measured according to Khan *et al.*, 2015. The level of GSH was expressed as μM .¹⁹

Measurement of lipid damage: Lipid damage was measured in terms of malonaldehyde (MDA) in the bacterial lysate using the modified method of Beuge and Aust.²⁰

Measurement of protein damage: To obtain the degree of protein carbonylation, derivatization was done with 2, 4 dinitrophenyl-hydrazine DNPH. The carbonyl concentration was calculated from the specific absorption at 370nm (relative to the reagent blank), the extinction coefficient of the protein-hydrazone complex being $22,000 \text{ M}^{-1}\text{cm}^{-1}$ and expressed as nmoles of carbonyl groups/mg protein.²¹

Measurement of Ni-uptake: Nickel uptake by selected test organisms was measured by atomic absorption spectroscopy following the protocol of Ronchini *et al.*, 2015.²²

In vitro radical scavenging assay:

Radical scavenging activity was measured by a decrease in absorbance at 517 nm of DPPH (2,2-Diphenyl-1-picrylhydrazyl) solution. To determine RSC of the metal complex and its respective ligand and inorganic nickel acetate, 1ml of DPPH (0.1mM) solution was mixed with 2ml of each test compound in methanol of varying concentration (1–15mg/ml) and kept for 20 minutes incubation in dark. After 20 minutes absorbance was measured at 517 nm. Decrease in the absorbance of the DPPH solution indicates an increase of the DPPH antioxidant activity and percentage of Radical Scavenging Activity (% RSC) was calculated by $(A_0 - A_s)/A_0 \times 100$ [A_0 = DPPH solution without the sample, A_s = DPPH solution with the sample].

Statistical analysis: All experiments were carried out in triplicate. Data obtained was analyzed by one-way analysis of variance, and mean was compared by Duncan's tests. Differences were considered significant at $P < 0.05$.

References

- 1 R. Rusakowicz, A. C. Testa, *J. Phys. Chem.*, 1968, **72**, 2680–2681.
- 2 J. V. Houten, R. J. Watts, *J. Am. Chem. Soc.*, 1976, **98**, 4853–4858.
- 3 G. M. Sheldrick, SHELXTL, v. 6.14; Bruker AXS Inc.: Madison, WI, **2003**.

- 4 C. K. Johnson, *ORTEP*, Report ORNL-5138, Oak Ridge National Laboratory, Oak Ridge, TN, **1976**.
- 5 C. Lee, W. Yang and R.G. Parr, *Phys. Rev. B*, 1998, **37**, 785–789.
- 6 M. J. Frisch, G. W. Trucks, H. B. Schlegel, G. E. Scuseria, M. A. Robb, J. R. Cheeseman, G. Scalmani, V. Barone, B. Mennucci, G. A. Petersson, H. Nakatsuji, M. Caricato, X. Li, H. P. Hratchian, A. F. Izmaylov, J. Bloino, G. Zheng, J. L. Sonnenberg, M. Hada, M. Ehara, K. Toyota, R. Fukuda, J. Hasegawa, M. Ishida, T. Nakajima, Y. Honda, O. Kitao, H. Nakai, T. Vreven, J. A. Montgomery, Jr., J. E. Peralta, F. Ogliaro, M. Bearpark, J. J. Heyd, E. Brothers, K. N. Kudin, V. N. Staroverov, R. Kobayashi, J. Normand, K. Raghavachari, A. Rendell, J. C. Burant, S. S. Iyengar, J. Tomasi, M. Cossi, N. Rega, J. M. Millam, M. Klene, J. E. Knox, J. B. Cross, V. Bakken, C. Adamo, J. Jaramillo, R. Gomperts, R. E. Stratmann, O. Yazyev, A. J. Austin, R. Cammi, C. Pomelli, J. W. Ochterski, R. L. Martin, K. Morokuma, V. G. Zakrzewski, G. A. Voth, P. Salvador, J. J. Dannenberg, S. Dapprich, A. D. Daniels, O. Farkas, J. B. Foresman, J. V. Ortiz, J. Cioslowski and D. J. Fox, *Gaussian 09 (Revision A.01)*, Gaussian, Inc., Wallingford CT, 2009.
- 7 (a) J. Autschbach, T. Ziegler, S. J. A. Gisbergen and E. J. Baerends, *J. Chem. Phys.*, 2002, **116**, 6930–6940; (b) K. L. Bak, P. Jørgensen, T. Helgaker, K. Rund and H. J. A. Jensen, *J. Chem. Phys.*, 1993, **98**, 8873–8887; (c) T. Helgaker and P. Jørgensen, *J. Chem. Phys.*, 1991, **95**, 2595–2601; (d) E. K. U. Gross and W. Kohn, *Adv. Quantum Chem.*, 1990, **21**, 255–291.
- 8 (a) M. Cossi, N. Rega, G. Scalmani and V. Barone, *J. Comput. Chem.*, 2003, **24**, 669–681; (b) M. Cossi and V. Barone, *J. Chem. Phys.*, 2001, **115**, 4708–471; (c) V. Barone and M. Cossi, *J. Phys. Chem. A*, 1998, **102**, 1995–2001.
- 9 (a) T. Liu, H. X. Zhang and B. H. Xia, *J. Phys. Chem. A*, 2007, **111**, 8724–8730; (b) A. Albertino, C. Garino, S. Ghiani, R. Gobetto, C. Nervi, L. Salassa, E. Rosenverg, A. Sharmin, G. Viscardi, R. Buscaino, G. Cross and M. Milanese, *J. Organomet. Chem.*, 2007, **692**, 1377–1391; (c) X. Zhou, H. X. Zhang, Q. J. Pan, B. H. Xia and A. C. Tang, *J. Phys. Chem. A*, 2005, **109**, 8809–8818; (d) X. Zhou, A. M. Ren and J. K. Feng, *J. Organomet. Chem.*, 2005, **690**, 338–347.
- 10 (a) P. J. Hay and W. R. Wadt, *J. Chem. Phys.*, 1985, **82**, 299–310; (b) P. J. Hay and W. R. Wadt, *J. Chem. Phys.*, 1985, **82**, 270–283
- 11 (a) M. S. Gordon, J. S. Binkley, J. A. Pople, W. J. Pietro and W. J. Hehre, *J. Am. Chem. Soc.*, 1982, **104**, 2797–2803; (b) J. S. Binkley, J. A. Pople and W. J. Hehre, *J. Am. Chem. Soc.*, 1980, **102**, 939–947.
- 12 N. M. O'Boyle, A. L. Tenderholt and K. M. Langner, *J. Comp. Chem.*, 2008, **29**, 839–845.

13. L. Xia, A. Idhayadhulla, Y. R. Lee, Y.-J. Wee and S. H. Kim, *Eur. J. Med. Chem.*, 2014, **86**, 605-612.
14. R.-F. Shang, G.-H. Wang, X.-M. Xu, S.-J. Liu, C. Zhang, Y.-P. Yi, J.-P. Liang and Y. Liu, *Molecules*, 2014, **19**, 19050-19065.
15. A. Mitra and K. Sarkar, *Manual of Modern Microbiology*, 1st Ed, Himalaya Publishing House, India, 2013.
16. M. Masoud, F. Ebrahimi and D. Minai-Tehrani, *J Mol Microbiol Biotechnol.*, 2014, **24**, 196–201.
17. X.-B. Fu, Z.-H. Lin, H.-F. Liu and X.-Y. Le., *Spectrochim. Acta A*, 2014, **122**, 22–33.
18. P. Jahangoshaei, L. Hassani, F. Mohammadi, A. Hamidi and K. Mohammadi, *J. Biol. Inorg. Chem.*, 2015, **20**, 1135–1146.
19. Z. Khan, M .A. Nisar, S. Z. Hussain, M. N. Arshad and A. Rehman, *Appl. Microbiol. Biotechnol.*, 2015, **99**, 10745–10757.
20. C. C. Otto, J. L. Koehl, D. Solanky and S. E. Haydel, *PLoS One*, 2014; **9**, e115172.
21. C. Pimentel, S. M. Caetano, R. Menezes, I. Figueira, C. N. Santos, R. B. Ferreira, M. A. Santos and C. Rodrigues-Pousada, *Biochim Biophys Acta*, 2014, **1840**, 1977-1986.
22. M . Ronchini, L. Cherchi, S. Cantamessa, M. Lanfranchi, A. Vianelli, P. Gerola, G. Berta and A. Fumagalli, *Environ. Sci Pollut Res Int.*, 2015, **22**, 7600-7611.

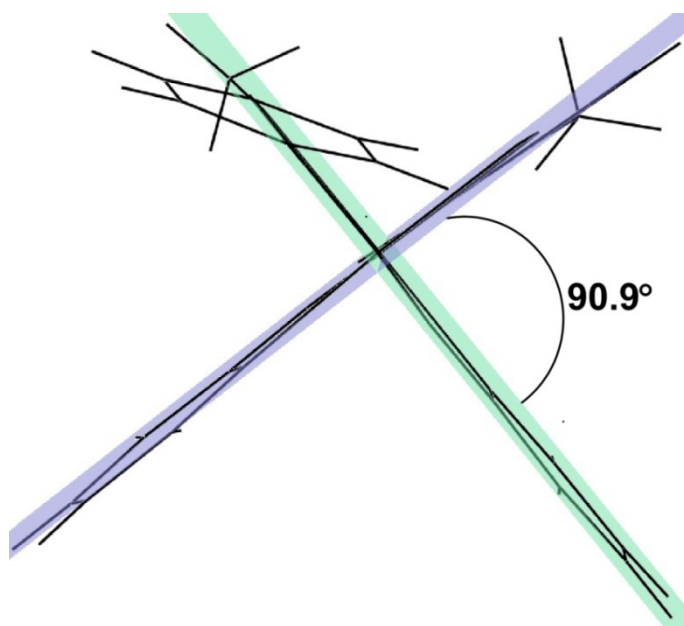


Fig. S1 Perpendicular disposition of the two coordinated ligand around Ni(II) in **2b**

Table S1 Summarized Crystallographic Data for **2b**

| | 2b |
|--|--|
| Empirical formula | C ₂₆ H ₂₂ N ₈ O ₂ Ni |
| fw | 537.20 |
| <i>T</i> /K | 298(2) |
| Cryst syst | Triclinic |
| Space group | <i>P</i> $\bar{1}$ |
| <i>a</i> /Å | 7.2755(3) |
| <i>b</i> /Å | 12.9036(5) |
| <i>c</i> /Å | 13.5575(5) |
| α /deg | 100.275(2) |
| β /deg | 92.818(2) |
| γ /deg | 96.958(2) |
| <i>V</i> /Å ³ | 1239.39(8) |
| <i>Z</i> | 2 |
| <i>D_c</i> /mgm ⁻³ | 1.418 |
| μ /mm ⁻¹ | 0.820 |
| <i>F</i> (000) | 556 |
| cryst size/mm ³ | 0.18×0.15×0.11 |
| θ /deg | 1.53–28.8 |
| measured reflns | 21940 |
| unique reflns, <i>R</i> _{int} | 6308, 0.0227 |
| GOF on <i>F</i> ² | 0.890 |
| <i>R</i> 1, ^a <i>wR</i> 2 ^b [<i>I</i> > 2σ(<i>I</i>)] | 0.0344, 0.1033 |
| <i>R</i> 1, <i>wR</i> 2(all data) | 0.0463, 0.1132 |

$$^aR1 = \frac{\sum |F_o| - |F_c|}{\sum |F_o|}$$

$$^b wR2 = [\sum w(F_o^2 - F_c^2)^2 / \sum w(F_o^2)^2]^{1/2}$$

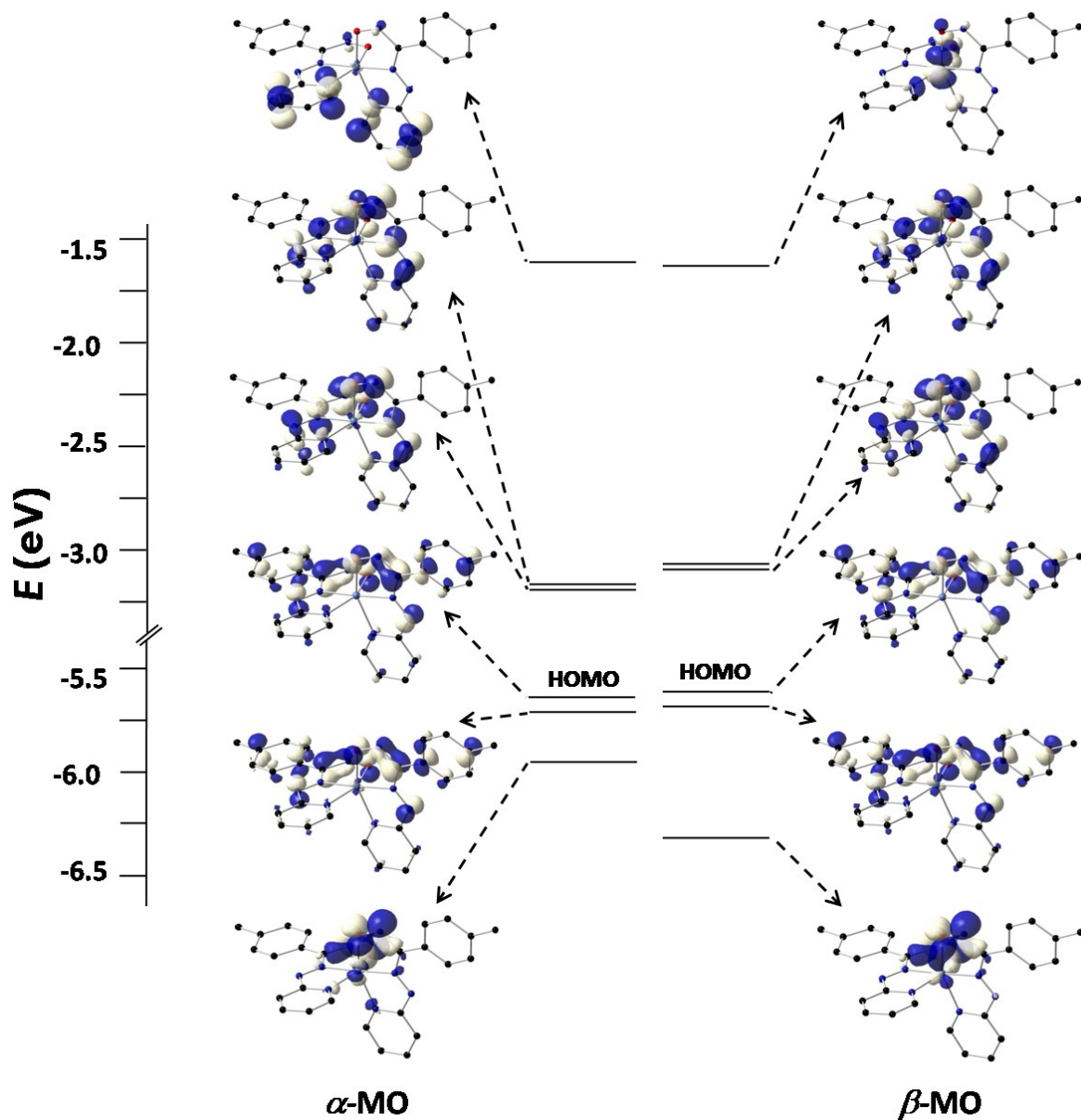


Fig. S2 Partial molecular orbital diagram and isodensity surface plots of some selected FMOs for complexes **2**. The arrows are intended to highlight the HOMO–LUMO energy gaps. All the DFT energy values are given in eV.

Table S2 Frontier Molecular Orbital Composition (%) in the Ground State for **2** ($S = 1$)

| Orbital | α -MO | Energy (eV) | Contribution (%) | | | | |
|---------|--------------|-------------|------------------|--------|----|-------|-------|
| | | | Ni | Ligand | | | |
| | | | | Azo | Py | Oxime | Tolyl |
| 141 | L+5 | -0.93 | 0 | 2 | 21 | 28 | 48 |
| 140 | L+4 | -0.96 | 1 | 3 | 28 | 25 | 43 |
| 139 | L+3 | -1.51 | 0 | 2 | 95 | 3 | 0 |
| 138 | L+2 | -1.58 | 1 | 2 | 89 | 6 | 2 |
| 137 | L+1 | -3.17 | 3 | 35 | 27 | 35 | 1 |
| 136 | LUMO | -3.18 | 2 | 34 | 27 | 36 | 1 |
| 135 | SOMO | -5.65 | 0 | 16 | 13 | 32 | 40 |
| 134 | H-1 | -5.71 | 1 | 15 | 12 | 30 | 42 |
| 133 | H-2 | -5.95 | 10 | 1 | 4 | 83 | 1 |
| 132 | H-3 | -5.99 | 12 | 32 | 3 | 50 | 3 |
| 131 | H-4 | -6.77 | 1 | 1 | 0 | 0 | 98 |
| 130 | H-5 | -6.77 | 0 | 0 | 0 | 0 | 99 |

| Orbital | β -MO | Energy (eV) | Contribution (%) | | | | |
|---------|-------------|-------------|------------------|--------|----|-------|-------|
| | | | Ni | Ligand | | | |
| | | | | Azo | Py | Oxime | Tolyl |
| 139 | L+5 | -1.31 | 67 | 15 | 4 | 11 | 4 |
| 138 | L+4 | -1.5 | 2 | 2 | 93 | 3 | 0 |
| 137 | L+3 | -1.57 | 2 | 2 | 89 | 5 | 2 |
| 136 | L+2 | -1.59 | 76 | 1 | 13 | 10 | 0 |
| 135 | L+1 | -3.09 | 3 | 33 | 25 | 37 | 1 |
| 134 | LUMO | -3.11 | 3 | 33 | 26 | 37 | 1 |
| 133 | SOMO | -5.64 | 0 | 16 | 13 | 31 | 39 |
| 132 | H-1 | -5.69 | 2 | 16 | 13 | 29 | 41 |
| 131 | H-2 | -6.29 | 16 | 2 | 2 | 78 | 2 |
| 130 | H-3 | -6.31 | 19 | 0 | 4 | 75 | 1 |
| 129 | H-4 | -6.77 | 0 | 0 | 0 | 0 | 99 |
| 128 | H-5 | -6.77 | 0 | 0 | 0 | 0 | 99 |

Table S3 Frontier Molecular Orbital Composition (%) in the Ground State for **3** ($S = 3/2$)

| Orbital | α -MO | Energy (eV) | Contribution (%) | | | | |
|---------|--------------|-------------|------------------|--------|----|-------|-------|
| | | | Ni | Ligand | | | |
| | | | | Azo | Py | Oxime | Tolyl |
| 142 | L+5 | 2.03 | 16 | 5 | 0 | 0 | 97 |
| 141 | L+4 | 1.77 | 1 | 3 | 37 | 10 | 50 |
| 140 | L+3 | 1.73 | 0 | 3 | 27 | 11 | 58 |
| 139 | L+2 | 1.61 | 0 | 1 | 76 | 10 | 13 |
| 138 | L+1 | 1.49 | 1 | 2 | 64 | 13 | 21 |
| 137 | LUMO | -0.29 | 2 | 34 | 26 | 37 | 1 |
| 136 | SOMO | -1.03 | 2 | 34 | 27 | 35 | 1 |
| 135 | H-1 | -2.55 | 9 | 5 | 7 | 75 | 4 |
| 134 | H-2 | -2.59 | 13 | 32 | 6 | 46 | 4 |
| 133 | H-3 | -2.73 | 2 | 14 | 16 | 49 | 19 |
| 132 | H-4 | -2.82 | 3 | 18 | 17 | 39 | 22 |
| 131 | H-5 | -3.56 | 32 | 19 | 9 | 34 | 6 |

| Orbital | β -MO | Energy (eV) | Contribution (%) | | | | |
|---------|-------------|-------------|------------------|--------|----|-------|-------|
| | | | Ni | Ligand | | | |
| | | | | Azo | Py | Oxime | Tolyl |
| 139 | L+5 | 1.89 | 12 | 2 | 12 | 15 | 60 |
| 138 | L+4 | 1.87 | 18 | 1 | 12 | 16 | 53 |
| 137 | L+3 | 1.7 | 1 | 2 | 95 | 1 | 1 |
| 136 | L+2 | 1.62 | 1 | 2 | 81 | 9 | 6 |
| 135 | L+1 | 0.45 | 3 | 31 | 30 | 33 | 3 |
| 134 | LUMO | 0.4 | 3 | 31 | 30 | 33 | 3 |
| 133 | SOMO | -2.47 | 0 | 20 | 20 | 39 | 21 |
| 132 | H-1 | -2.54 | 3 | 19 | 19 | 38 | 22 |
| 131 | H-2 | -2.86 | 17 | 1 | 1 | 80 | 1 |
| 130 | H-3 | -2.89 | 19 | 0 | 3 | 77 | 0 |
| 129 | H-4 | -3.85 | 16 | 66 | 0 | 15 | 3 |
| 128 | H-5 | -4.17 | 13 | 15 | 25 | 0 | 46 |

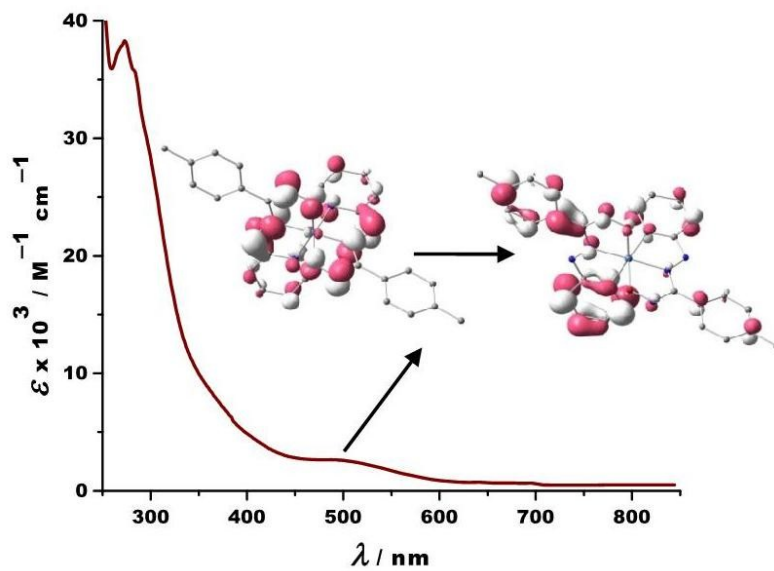


Figure S3 Experimental absorption spectra of 3 in dichloromethane solution.

Table S4 Main optical transition at the TD-DFT/B3LYP Level for the complex **2** with composition in terms of molecular orbital contribution of the transition, Computed Vertical excitation energies, and oscillator strength in dichloromethane

| Transition | CI | Composition | E (eV) | Oscillator strength (<i>f</i>) | λ_{theo} (nm) |
|--------------------------|---------------------|--|------------|----------------------------------|------------------------------|
| $S_0 \rightarrow S_{16}$ | 0.49638 0.49263 | H - 1(A) \rightarrow L + 1(A) (37%) H - 1(B) \rightarrow L + 1(B) (35%) | 2.302 8 | 0.1688 | 538.4 0 |
| $S_0 \rightarrow S_{17}$ | 0.59242 0.48666 | H - 1(A) \rightarrow L (A) (52%) H - 1(B) \rightarrow L (B) (46%) | 2.309 3 | 0.2192 | 536.9 0 |
| $S_0 \rightarrow S_9$ | 0.63480 | H - 6 \rightarrow L (81%) | 2.813 6 | 0.0430 | 440.6 6 |
| $S_0 \rightarrow S_{59}$ | -0.47848 0.45284 | H (A) \rightarrow L + 2(A) (32%) H (B) \rightarrow L + 3(B) (31%) | 3.793 1 | 0.3935 | 326.8 7 |
| $S_0 \rightarrow S_{86}$ | 0.52484 0.50886 | H (A) \rightarrow L + 4(A) (28%) H (B) \rightarrow L + 6(B) (26%) | 4.264 8 | 0.1346 | 290.7 1 |
| $S_0 \rightarrow S_{87}$ | 0.60786 -0.55434 | H (A) \rightarrow L + 5(A) (37%) H (B) \rightarrow L + 7(B) (31%) | 4.269 7 | 0.2778 | 290.3 8 |

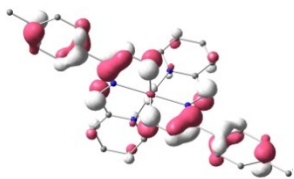
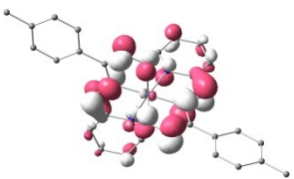
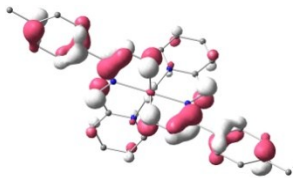
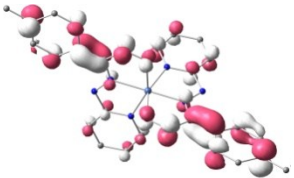
| λ_{expt} (nm) | | Hole | Electron |
|---------------------------------|-----------------|---|--|
| | S_{17} | | |
| | w = 0.70 | | |
| 509 | 2.3093 (0.2192) |  |  |
| nm | 536.90 nm | | |
| | ILCT | | |
| | S_{86} | | |
| | w = 0.55 | | |
| 275 | 4.2648 (0.1346) |  |  |
| nm | 290.71 | | |
| | ILCT/MLCT | | |

Fig. S4 Natural transition orbitals (NTOs) for complex **2** illustrating the nature of singlet excited states in the absorption bands in the range 250–600 nm. For each state, the respective number of the state, transition energy (eV), and the oscillator strength (in parentheses) are listed. Shown are only occupied (holes) and unoccupied (electrons) NTO pairs that contribute more than 55% to each excited state.

Table S5 Main optical transition at the TD-DFT/B3LYP Level for the complex **3** with composition in terms of molecular orbital contribution of the transition, Computed Vertical excitation energies, and oscillator strength in dichloromethane

| Transition | CI | Composition | E (eV) | Oscillator strength (<i>f</i>) | λ_{theo} (nm) |
|--------------------------|---------|-------------------------------------|--------|----------------------------------|------------------------------|
| $S_0 \rightarrow S_{18}$ | 0.69876 | H (A) \rightarrow L + 4 (A) (49%) | 2.4882 | 0.1258 | 498.29 |
| $S_0 \rightarrow S_{19}$ | 0.58957 | H (A) \rightarrow L + 3 (A) (35%) | 2.5130 | 0.1359 | 493.37 |
| $S_0 \rightarrow S_{91}$ | 0.49849 | H (B) \rightarrow L + 6 (B) (25%) | 4.1353 | 0.0419 | 299.82 |

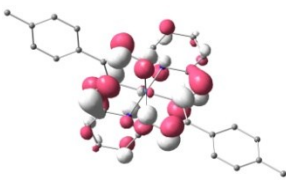
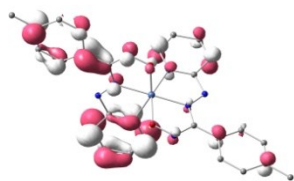
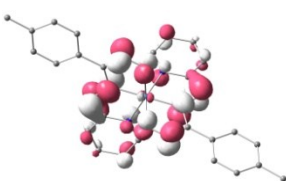
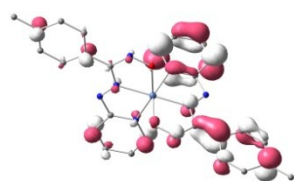
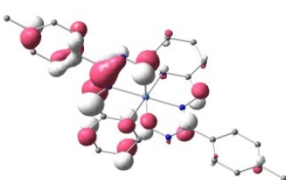
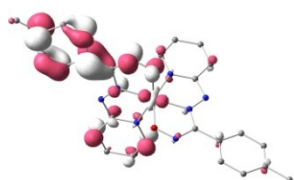
| λ_{expt} (nm) | | Hole | Electron |
|---------------------------------|--|--|---|
| | S_{18} | | |
| 509 | $w = 0.87$ |  |  |
| nm | 2.4882 (0.1258) | | |
| | 498.29 nm | | |
| | ILCT/LLCT | | |
| | S_{19} | | |
| | $w = 0.70$ |  |  |
| | 2.5130 (0.1359) | | |
| | 493.37 nm | | |
| | ILCT/LLCT | | |
| | $\pi(\text{py} + \text{azo} + \text{oxime}) \rightarrow \pi^*(\text{py} + \text{tolyl} + \text{azo} + \text{oxime})$ | | |
| | S_{91} | | |
| 275 | $w = 0.49$ |  |  |
| nm | 4.1353 (0.0419) | | |
| | 299.82 | | |
| | ILCT/LLCT | | |

Fig. S5 Natural transition orbitals (NTOs) for complex **3** illustrating the nature of singlet excited states in the absorption bands in the range 250–600 nm. For each state, the respective number of the state, transition energy (eV), and the oscillator strength (in parentheses) are listed. Shown are only occupied (holes) and unoccupied (electrons) NTO pairs that contribute more than 50% to each excited state.

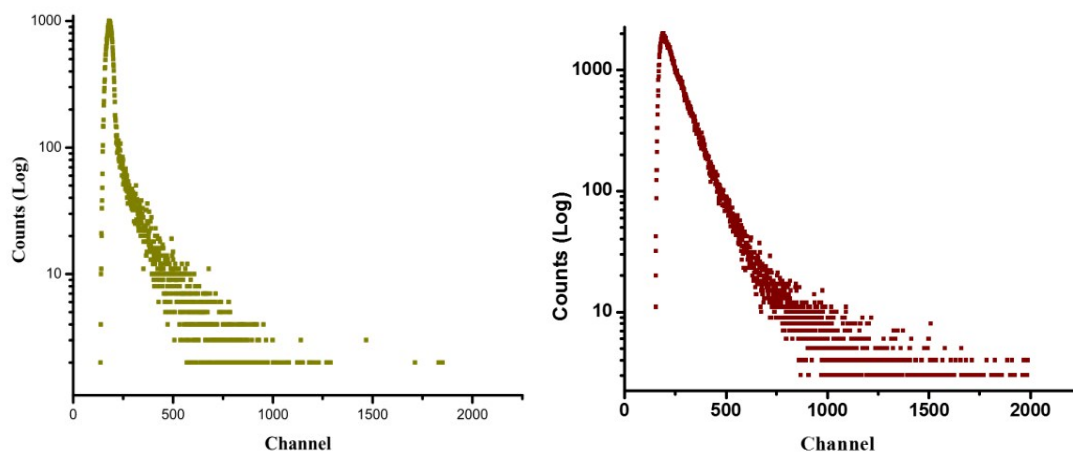


Fig. S6 Changes in the time-resolved photoluminescence decay of complexes **2**(left) and **3** (right) in CH_2Cl_2 at room temperature obtained with 330 nm excitation. The emission at 409 and 410 nm was monitored for complex **2** and **3** respectively.

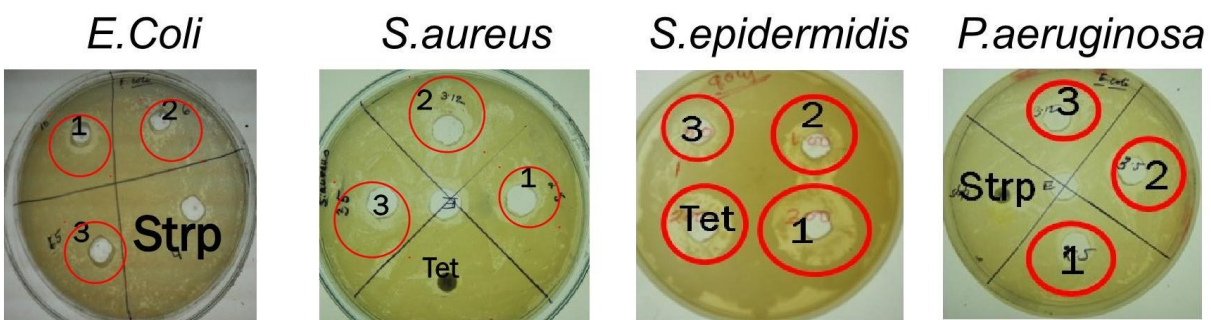


Fig. S7 Agar cup plate assay showing ZOI. 1 indicates treatment with IC₅₀ of Ni(II) complex, 2 indicates IC₅₀ dose of free ligand 3 indicates treatment with IC₅₀ of nickel acetate. Tet= tetracyclin, strp = streptomycin.

Table S6 Effect of IC₅₀ dose of synthesized nickel azo-oxime complex, free ligand and nickel acetate on antioxidant enzymes of tested bacteria

| | <i>E.coli</i> | <i>P.aeruginosa</i> | <i>S.aureus</i> | <i>S.epidermidis</i> |
|---------------------------------|---------------|---------------------|-----------------|----------------------|
| Catalase (U/mg protein) | | | | |
| Cont | 0.82±0.05 | 0.39±0.02 | 2.9± 0.03 | 1.5±0.08 |
| Nickel(II) complex, 2 | 0.5±0.03*** | 0.2±0.03*** | 1.2±0.02*** | 0.5±0.03*** |
| Azo-oxime ligand, 1 | 0.65±0.03** | 0.36±0.05* | 2.1±0.03** | 1.2±0.08** |
| Nickel acetate | 0.60±0.03** | 0.30±0.03** | 2.5±0.03** | 1.25±0.03** |
| SOD (U/mg protein) | | | | |
| Cont | 18.5±0.73 | 13.56±0.58 | 21.7±0.9 | 15.6±0.89 |
| Nickel(II) complex, 2 | 7.2±0.6*** | 6.6±0.95*** | 9.5±1.1*** | 8.4±0.6*** |
| Azo-oxime ligand, 1 | 12.5± 1.2*** | 10.6± 0.85** | 12.5± 1.2*** | 10.2±1*** |
| Nickel acetate | 11.2± 1.2*** | 10.1±0.6*** | 14.5± 1.0*** | 11.2± 0.9*** |
| Peroxidase(U/mg protein) | | | | |
| Cont | 0.88± 0.02 | 0.48±0.01 * | 0.69±0.03 | 0.5±0.02 |
| Nickel(II) complex, 2 | 0.52±0.02** | 0.24±0.03** | 0.3±0.02*** | 0.3±0.01*** |
| Azo-oxime ligand, 1 | 0.72±0.03** | 0.41±0.5* | 0.55±0.03** | 0.38±0.0* |
| Nickel acetate | 0.81±0.3* | 0.38±0.4* | 0.65± 0.05* | 0.4± 0.03* |

All values are expressed as mean ± SD (*Indicates p<0.05, **indicates p<0.01 ***indicates P<0.001)

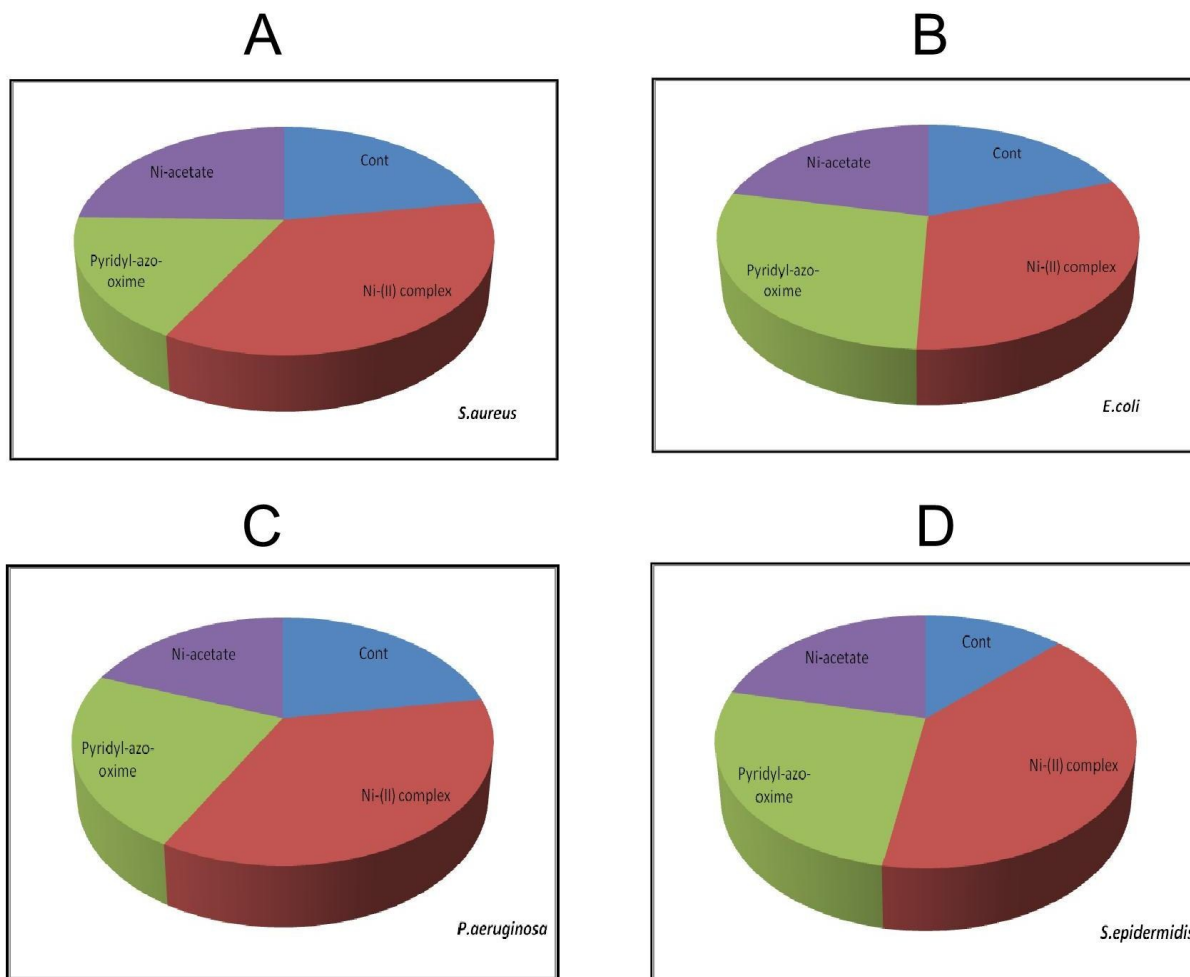


Fig. S8 Effect of IC₅₀ dose of nickel complex **2**, free ligand **1** and nickel acetate on lipid peroxidation level in all tested bacteria (All values expressed as mean ± SD)

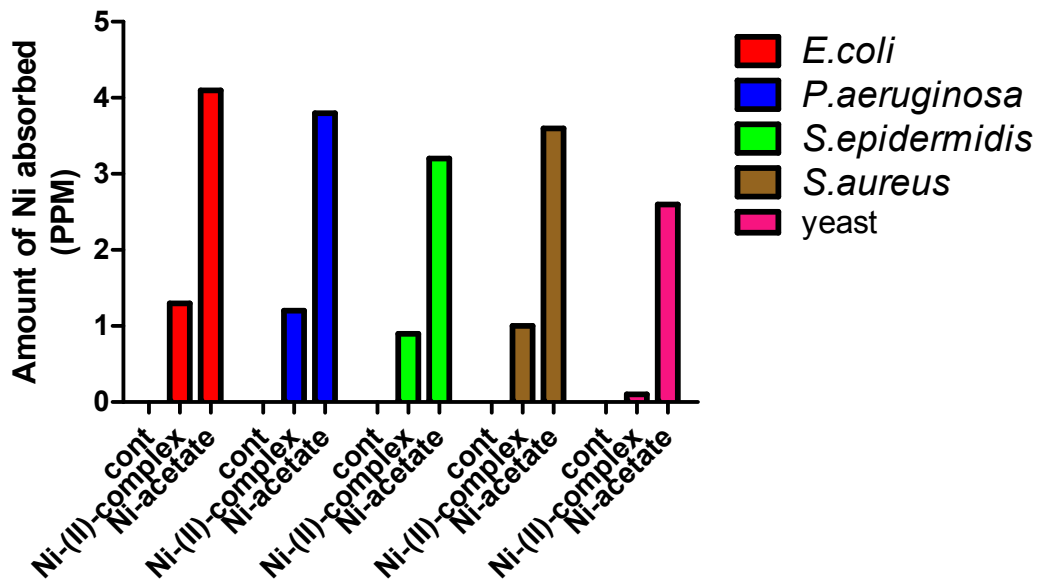


Fig. S9 Analysis of nickel uptake by tested organisms.

Table S7 Coordinates of optimized geometry **2b**

| Tag | Symbol | X | Y | Z |
|------------|---------------|----------|----------|----------|
| 1 | Ni | 0.000259 | 0.054389 | -0.00172 |
| 2 | N | -0.21483 | 1.494874 | -1.57453 |
| 3 | C | 0.693115 | 2.253779 | -2.19978 |
| 4 | H | 1.716515 | 2.162294 | -1.84477 |
| 5 | C | 0.368144 | 3.114255 | -3.24754 |
| 6 | H | 1.141255 | 3.707772 | -3.72433 |
| 7 | C | -0.96849 | 3.181915 | -3.65956 |
| 8 | H | -1.26154 | 3.839173 | -4.47375 |
| 9 | C | -1.9191 | 2.395978 | -3.01899 |
| 10 | H | -2.96597 | 2.407187 | -3.30277 |
| 11 | C | -1.51012 | 1.551518 | -1.97229 |
| 12 | N | -2.48151 | 0.760852 | -1.35195 |
| 13 | N | -1.9845 | 0.010861 | -0.42589 |
| 14 | C | -2.71341 | -0.85613 | 0.318634 |
| 15 | C | -4.16625 | -1.13209 | 0.261703 |
| 16 | C | -5.02667 | -0.57277 | -0.70142 |
| 17 | H | -4.63212 | 0.10021 | -1.44911 |
| 18 | C | -6.39087 | -0.88114 | -0.70456 |
| 19 | H | -7.02671 | -0.43302 | -1.4657 |
| 20 | C | -6.95379 | -1.74631 | 0.238545 |
| 21 | C | -6.0922 | -2.30268 | 1.20001 |
| 22 | H | -6.49317 | -2.98165 | 1.950621 |
| 23 | C | -4.73403 | -2.00881 | 1.215419 |
| 24 | H | -4.09548 | -2.45859 | 1.966693 |
| 25 | C | -8.42774 | -2.07873 | 0.231997 |
| 26 | H | -8.90317 | -1.80836 | 1.183861 |
| 27 | H | -8.59377 | -3.15388 | 0.084117 |
| 28 | H | -8.95431 | -1.54691 | -0.56775 |
| 29 | N | -1.99642 | -1.56131 | 1.243876 |
| 30 | O | -0.74187 | -1.36772 | 1.328441 |
| 31 | N | 0.214722 | 1.496528 | 1.56924 |
| 32 | C | -0.69378 | 2.250864 | 2.199184 |
| 33 | H | -1.71839 | 2.154612 | 1.849059 |
| 34 | C | -0.36821 | 3.112297 | 3.245994 |
| 35 | H | -1.14202 | 3.70195 | 3.726426 |
| 36 | C | 0.96984 | 3.185691 | 3.652517 |
| 37 | H | 1.263384 | 3.843424 | 4.466131 |
| 38 | C | 1.920995 | 2.403936 | 3.007618 |
| 39 | H | 2.968668 | 2.417912 | 3.288263 |
| 40 | C | 1.511294 | 1.55846 | 1.962035 |
| 41 | N | 2.483746 | 0.77253 | 1.337625 |
| 42 | N | 1.985925 | 0.016682 | 0.416662 |
| 43 | C | 2.714167 | -0.85538 | -0.32251 |
| 44 | C | 4.166152 | -1.13492 | -0.26063 |
| 45 | C | 5.057589 | -0.43407 | 0.573178 |
| 46 | H | 4.686763 | 0.349156 | 1.218515 |
| 47 | C | 6.421329 | -0.74419 | 0.580791 |

| | | | | |
|----|---|----------|----------|----------|
| 48 | H | 7.082019 | -0.18217 | 1.238189 |
| 49 | C | 6.952567 | -1.75366 | -0.22764 |
| 50 | C | 6.059705 | -2.45289 | -1.05851 |
| 51 | H | 6.435607 | -3.24755 | -1.70067 |
| 52 | C | 4.702154 | -2.1564 | -1.07902 |
| 53 | H | 4.039399 | -2.71537 | -1.72916 |
| 54 | C | 8.424895 | -2.09252 | -0.21152 |
| 55 | H | 8.981166 | -1.42739 | 0.457691 |
| 56 | H | 8.866429 | -2.0069 | -1.21285 |
| 57 | H | 8.593253 | -3.12343 | 0.126731 |
| 58 | N | 1.996133 | -1.56692 | -1.24206 |
| 59 | O | 0.741675 | -1.37303 | -1.32719 |

Table S7 Coordinates of optimized geometry **3b**

| Tag | Symbol | X | Y | Z |
|------------|---------------|----------|----------|----------|
| 1 | Ni | 0.003842 | 0.003566 | -0.05716 |
| 2 | N | -0.17077 | 1.784316 | 1.137557 |
| 3 | C | 0.766173 | 2.518094 | 1.750243 |
| 4 | H | 1.777893 | 2.120699 | 1.703003 |
| 5 | C | 0.494394 | 3.711702 | 2.412926 |
| 6 | H | 1.292388 | 4.263118 | 2.900552 |
| 7 | C | -0.83801 | 4.169943 | 2.422384 |
| 8 | H | -1.09578 | 5.101336 | 2.922321 |
| 9 | C | -1.81784 | 3.429646 | 1.785339 |
| 10 | H | -2.85544 | 3.747914 | 1.757147 |
| 11 | C | -1.46655 | 2.218658 | 1.13597 |
| 12 | N | -2.45258 | 1.504144 | 0.501855 |
| 13 | N | -1.97361 | 0.447142 | -0.12279 |
| 14 | C | -2.73595 | -0.42693 | -0.81604 |
| 15 | C | -4.20312 | -0.39956 | -1.02657 |
| 16 | C | -5.04492 | 0.614345 | -0.52903 |
| 17 | H | -4.61178 | 1.425148 | 0.040012 |
| 18 | C | -6.42478 | 0.583784 | -0.76456 |
| 19 | H | -7.04174 | 1.387653 | -0.36394 |
| 20 | C | -7.02749 | -0.44323 | -1.4965 |
| 21 | C | -6.18705 | -1.4543 | -1.99545 |
| 22 | H | -6.61723 | -2.27194 | -2.57375 |
| 23 | C | -4.81495 | -1.43705 | -1.77067 |
| 24 | H | -4.18941 | -2.22793 | -2.16825 |
| 25 | C | -8.51892 | -0.47524 | -1.74547 |
| 26 | H | -8.98373 | -1.36943 | -1.3068 |
| 27 | H | -8.75002 | -0.4892 | -2.81962 |
| 28 | H | -9.01346 | 0.401594 | -1.31115 |
| 29 | N | -2.07732 | -1.48482 | -1.37416 |
| 30 | O | -0.79446 | -1.5281 | -1.24427 |
| 31 | N | 0.155603 | -1.34705 | 1.610346 |
| 32 | C | -0.79006 | -1.86077 | 2.406182 |
| 33 | H | -1.80031 | -1.49842 | 2.227309 |
| 34 | C | -0.52916 | -2.79362 | 3.405607 |
| 35 | H | -1.33413 | -3.17084 | 4.028754 |
| 36 | C | 0.802586 | -3.2234 | 3.571794 |
| 37 | H | 1.052685 | -3.95587 | 4.336499 |
| 38 | C | 1.791271 | -2.71138 | 2.751172 |
| 39 | H | 2.828665 | -3.02003 | 2.83547 |
| 40 | C | 1.450993 | -1.75771 | 1.757859 |
| 41 | N | 2.445655 | -1.26892 | 0.949042 |
| 42 | N | 1.977652 | -0.44396 | 0.033086 |
| 43 | C | 2.750033 | 0.180522 | -0.88306 |
| 44 | C | 4.216022 | 0.07148 | -1.07489 |
| 45 | C | 5.034399 | -0.81371 | -0.34646 |
| 46 | H | 4.584823 | -1.44676 | 0.405643 |

| | | | | |
|----|---|----------|----------|----------|
| 47 | C | 6.412205 | -0.88082 | -0.58518 |
| 48 | H | 7.010793 | -1.58053 | -0.00263 |
| 49 | C | 7.035779 | -0.08052 | -1.54666 |
| 50 | C | 6.219347 | 0.804446 | -2.27305 |
| 51 | H | 6.667033 | 1.445746 | -3.03219 |
| 52 | C | 4.849178 | 0.881205 | -2.04825 |
| 53 | H | 4.241337 | 1.568737 | -2.62515 |
| 54 | C | 8.524147 | -0.15811 | -1.80424 |
| 55 | H | 9.004842 | -0.88696 | -1.14117 |
| 56 | H | 9.014922 | 0.811901 | -1.64331 |
| 57 | H | 8.740651 | -0.45798 | -2.83913 |
| 58 | N | 2.104984 | 1.036365 | -1.72838 |
| 59 | O | 0.821457 | 1.128956 | -1.62264 |